Hyporheic water exchange in a large hydropower-regulated boreal river – directions and rates

D. Siergieiev, A. Lundberg and A. Widerlund

ABSTRACT

Widespread river regulation is known to modify river-aquifer interactions, influencing entire watersheds, but knowledge of the hyporheic flowpath along regulated rivers is limited. This study measured the hydraulic conductivity of the river bed and the aquifer, water levels and seepage fluxes in the heavily regulated Lule River in Northern Sweden, with the aim of characterising water exchange across the river-aquifer interface. While pristine rivers in the area are gaining, the Lule River was recharging the aquifer during 10% of the time. Daily river level fluctuations (typically ±0.25 m) directed ~3% of the total orthogonal flux across the river bed towards the aquifer, while during ~2% of the time the orthogonal fluxes were negligible ($\leq 10^{-4}$ m d^{-1}). A clogging layer on the river bed, most likely formed due to the modified river discharge, restricted river-aquifer exchange. The hyporheic zone had higher electrical conductivity than the river and the aquifer and electrical conductivity occasionally decreased following rising river water levels, with 3–5 hours' delay. Overall, hydropower regulation has severely altered the hydrological regime of the hyporheic zone in the Lule River.

Key words | clogging layer, connectivity, hyporheic, regulated, riparian, water level

D. Siergieiev (corresponding author)
A. Lundberg
A. Widerlund
Lulea University of Technology,
SE-971 87 Lulea,
Sweden
E-mail: *dmysie@ltu.se*

INTRODUCTION

Pristine rivers in Northern Sweden are recharged by groundwater throughout most of the year, and corridors adjacent to these rivers are thus mainly characterised by groundwater. This creates fairly uniform conditions with relatively stable temperature, redox and pH gradient just under and along the river, i.e. in the hyporheic zone. Most of the exchange between river and groundwater takes place in the hyporheic zone (Wondzell 2011). Natural floods can drastically change the flow pattern in the hyporheic zone, increasing the fraction of river water in the subsurface layer. Good connectivity between pristine rivers and groundwater is maintained by the prevailing groundwater outflow into the river and by the distinct flow peaks induced by rainfall and snowmelt events, which remove fine particles from the river bed (Hancock 2002; Hanrahan 2008).

River-groundwater connectivity can be severely altered when the spring flood is damped and river water is forced in and out the aquifer in an unnatural way as a result of regulation (Arntzen *et al.* 2006). Globally, roughly 66% of rivers are regulated in some way for human activities, while in Scandinavia 84% of rivers with mean annual discharge above 40 m^3 s^{-1} are regulated (Dynesius & Nilsson 1994; Nilsson *et al.* 2005). Fragmentation by dams has the most widespread impact on rivers (Jansson *et al.* 2000), resulting in river ecosystems being among the most threatened in the world (Renöfält *et al.* 2010). As a result of efforts to reduce emissions of greenhouse gases by phasing out fossil fuels, additional pressure on rivers can be expected through increased demand for hydropower (Zhao *et al.* 2012). This will lead in turn to further disturbance of hyporheic processes (Humborg *et al.* 2008).

The hyporheic process in natural systems is well documented and it is known that the interaction between surface water and groundwater occurs in response to, for example, variations in river discharge, bed topography and hydraulic conductivity of the river bed and the aquifer.

doi: 10.2166/nh.2013.011

The extent of the hyporheic zone varies with stream order, characteristics of the river and season (Howard *et al.* 2006; Wondzell 2011). The hyporheic zone is an important habitat for hyporheos, i.e. invertebrates, stygobites, salmonids, etc. (Dole-Olivier 2011). Hyporheic water exchange plays a crucial role in controlling the hyporheic assemblage by damping the physico-chemical variations that occur as a function of sediment permeability, oxygen concentration, nutrient status and thermal conditions (Murray *et al.* 2008). The hyporheic zone represents a transition between the river and the riparian zone, which connects in turn aquatic and terrestrial ecosystems.

Despite their importance, studies of hyporheic processes along regulated rivers are rare (Hanrahan 2008) and most are fairly recent (Arntzen *et al.* 2006; Sawyer *et al.* 2009; Gerecht *et al.* 2011; McDonald *et al.* 2012). Hyporheic exchange in regulated environments is reported to be heterogeneous due to the unnatural flow pattern (Hancock & Boulton 2005; Hanrahan 2008; Gibbins *et al.* 2009). Overall deterioration of vertical connectivity, the degree of temporal instability in the hyporheic zone and alteration of groundwater levels and hyporheic flow directions are all the result of changes in river discharge (Arntzen *et al.* 2006; Calles *et al.* 2007; Sawyer *et al.* 2009; Francis *et al.* 2010) and groundwater flux towards the river (Howard *et al.* 2006). Water fluxes across the river-aquifer interface in regulated rivers result in high variability in hyporheic heat and nutrient fluxes (Arntzen *et al.* 2006; Sawyer *et al.* 2009), which can compromise hyporheos and spawning processes (Soulsby *et al.* 2001; Geist *et al.* 2008). Hyporheic biogeochemical processes may also be affected by increased residence time in the hyporheic zone, which was recently related to frequent low-amplitude river discharge fluctuations (Maier & Howard 2011). As a whole, regulation of rivers promotes degradation of the river floodplain and its riparian and hyporheic zones (Zhao *et al.* 2012).

The effects of river regulation on the hyporheic zone have only recently attracted research interest, and there is thus a lack of background material for the planned revision of the European Commission's Groundwater Directive (Directive 2006/118/EC). The present study forms part of the large-scale, integrated EU project GENESIS (Klöve 2008), which aims to provide a scientific basis and technical guidance for updating the Groundwater Directive.

This study was performed in the Lule River in the boreal part of Northern Sweden, where spring snowmelt causes the highest discharge peaks in natural rivers and winter base flow is dominated by groundwater. However, studies of the flow pattern of this heavily regulated river indicate relatively low spring peaks and high winter flow, with frequent short-term water level fluctuations during summer. This altered river discharge is likely to impair river-aquifer connectivity and promote colmation of the river bed (Brunke & Gonser 1997; Blaschke *et al.* 2003).

Given the lack of previous studies and the fact that hyporheic and riparian zones are exposed to risk as a result of river regulation, this study sought to assess and quantify hyporheic hydrological processes in the heavily regulated Lule River and to determine the implications for the biogeochemical function of hyporheic exchange flows.

RIVER BASIN

The Lule River originates in the Scandinavian Caledonides in Northern Sweden and flows 460 km southeast towards the Bothnian Bay in the Baltic Sea (Figure 1). The climate is sub-arctic, with annual precipitation gradually decreasing from 1,000–1,500 to 400–700 mm (of which ~45% falls as snow) from Caledonides to coast, while annual evapotranspiration increases from 100 to 300 mm along the same stretch (Raab & Vedin 1995). The river has a catchment area of 25,110 km^2 and mean annual discharge of 506 $m^3 s^{-1}$. The ice cover period is typically five months, from November to April (Raab & Vedin 1995).

The Lule River is obstructed by 15 dams and more than 70% of its annual runoff can be stored in reservoirs. This is the highest live storage (water volume that can be used for regulation) among Eurasian rivers (Dynesius & Nilsson 1994). The discharge pattern is characterised by a diminished spring peak (delayed by about one month), elevated water release during winter and daily water level fluctuations in response to diurnal electricity demand during summer. The regional groundwater regime in the catchment has its minimum just prior to and its maximum after snowmelt (May) and decays continuously from mid-summer to late spring (April). However, close to the coast an autumn peak may occur due to rain events (Aneblom *et al.* 2005).

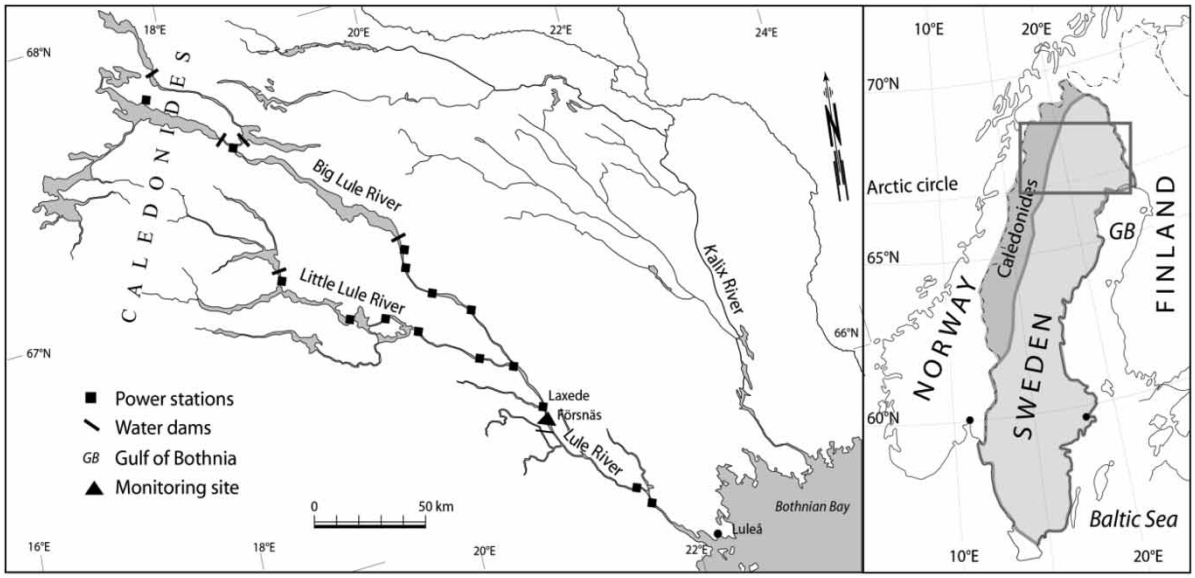

Figure 1 | Map showing the location of the study site in the Lule River.

MATERIALS AND METHODS

Monitoring site

The monitoring site was located 100 km upstream from the river mouth, below Laxede power station (N66°11.67′; E20°52.32′) (Figure 1). Daily water release from the power station upstream and damming by the downstream reservoir cause the river water level to vary typically within ±0.25 m at the site. Glaciofluvial and alluvial sediments with layers of loam dominate in the hyporheic zone at the site, with coarse sand in deeper horizons (Figure 2). The average thickness of the alluvial sediment sequence is ~10 m. At the test site, the river is approximately 300 m wide and 10 m deep, with the gently sloping bed mainly composed of ~0.3 m thick silty material formed as a result of colmation processes induced by river regulation (Blaschke *et al.* 2003; Rehg *et al.* 2005; Nogaro *et al.* 2010). Large pebbles and boulders are common within the river bed sediments.

Monitoring equipment

A measurement profile orthogonal to the river was established, with five monitoring stations: one in the river and four groundwater wells on land at 1, 2, 5 and 25 m from the mean shore line (MSL) (Figure 2). The wells nearest to the MSL (L1 and L2) were 1.7 m deep and 2.5 cm in diameter, whereas wells L5 and L25 were 2.7 and 4.3 m deep, respectively, and 5 cm in diameter. All wells were screened 1 m from the bottom.

Time series data on water level, temperature and electrical conductivity were collected at the river and in wells L5 and L25, using dataloggers recording momentary data every 15 min, while only temperature and electrical conductivity were measured in wells L1 and L2. The measuring sensors (Table 1) were installed approximately 0.1 m from the bottom of the wells. The temperature and electrical conductivity data were checked against data obtained using a manual water quality probe (Hydrolab Surveyor II) and were calibrated twice during the monitoring period, which ran from June to October 2012.

A vertical profile with temperature sensors distributed at 0.2 to 0.3 m intervals down to 1.0 was installed in the river bed, 2 m from the MSL and another to 2.7 m depth at a point 5 m inland from the MSL (Figure 2). Recording occurred every 15 min.

Hyporheic zone characterisation

Hyporheic exchange was described using the hydraulic conductivity of the river bed and the aquifer, the hydraulic

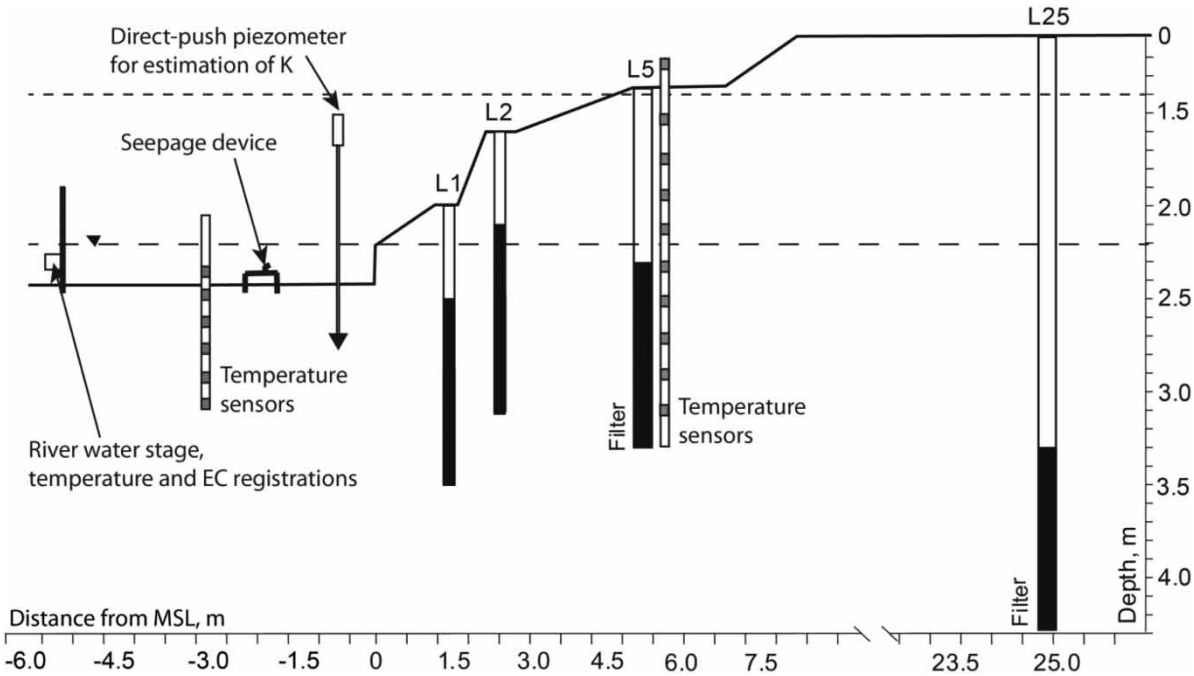

Figure 2 | Monitoring site for the Lule River. Short dashed line – maximum observed river water and groundwater levels; long dashed line – mean river and groundwater levels; solid line – ground surface. Well number (L1-L25) indicates the distance in metres from the mean shore line (MSL). Sites of temperature profile sensors, seepage meters and direct-push piezometer installations are shown.

Table 1 | Specifications of the sensors used for continuous monitoring

Parameter	Operating range	Accuracy	Sensor	Manufacturer
Water level	0–5 m	± 3.1 mm	STS PTM/N	Sensor Technik Sirnach AG
Electrical conductivity	0–200 μS cm^{-1}	±0.1 μS cm^{-1}	WQ-Cond-1	Global Water
Temperature in gw wells	−5–70 °C	±0.01 °C		
Temperature depth profiles	−20–50 °C	< ± 0.4 °C	UA-001-64	Onset Hobo Dataloggers

gradient across the river bed, recorded temperature and the electrical conductivity of the river and the aquifer.

The hydraulic conductivity of the aquifer K_{aq} (m d^{-1}) was determined by slug test using the methods proposed by Hvorslev (1951) and Bouwer and Rice (Bouwer 1989) (Figure 3(a)).

The hydraulic conductivity of the clogging layer K_{cl} (m d^{-1}) was determined by a varying pressure head infiltration method using a direct-push piezometer (Figure 3(b)) (Hvorslev 1951; Ronkanen & Klove 2005). The test was performed at 0.1 m depth intervals down to 0.7 m depth in the river bed, on two occasions. The measurements were made at 1.0 and 2.5 m from the MSL and hydraulic conductivity was calculated as:

$$K_{cl} = \ln\left(\frac{H_0 - h}{H_0 - H}\right)\frac{\pi R^2}{Ft} \quad (1)$$

where H (m) is the initial water level in the reservoir, h (m) is the water level at time t (s), H_0 (m) is the distance from the river water surface to the tip of the piezometer, and R (m) is the radius of the reservoir. The shape factor F (–) was calculated as $F \approx -5.5r$, where r is the radius of the piezometer (Hvorslev 1951).

For orthogonal flow across the river bed, the equivalent hydraulic conductivity K_E (m d^{-1}) was calculated to account

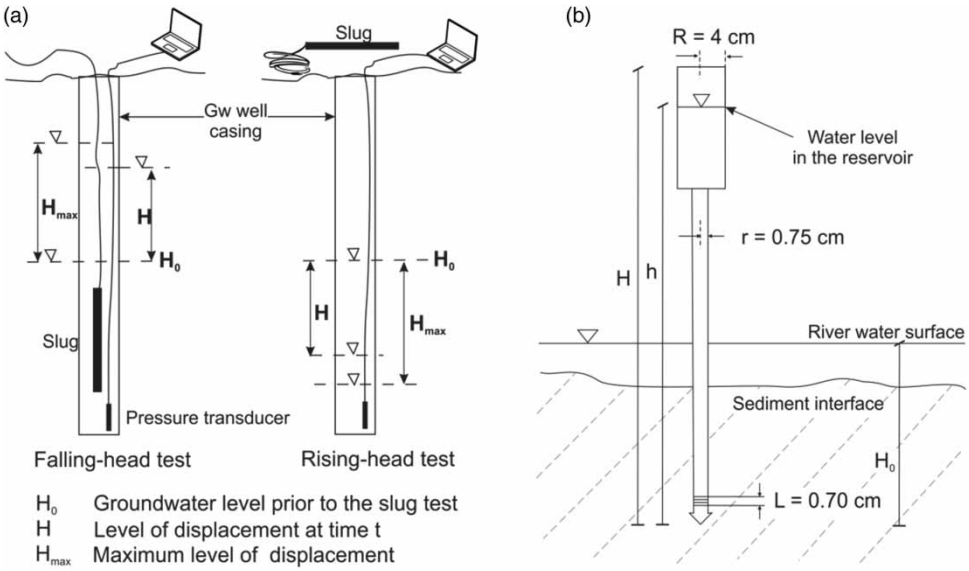

Figure 3 | Devices used for determination of hydraulic conductivity (K). (a) Slug test for the aquifer (K_{aq}); (b) direct-push piezometer for the clogging layer (K_{cl}).

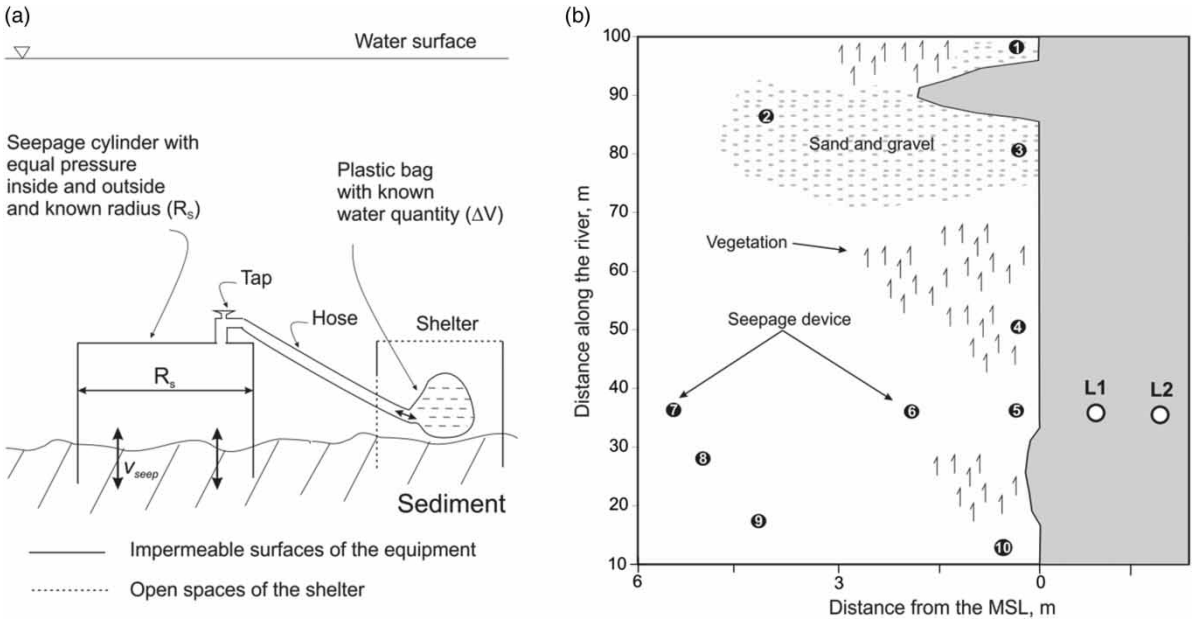

Figure 4 | (a) Device used for assessment of spatial variation in seepage flow and determination of mean equivalent hydraulic conductivity (K_E) for the aquifer and the clogging layer; (b) location of the seepage devices and observation wells L1 and L2.

for differing hydraulic conductivity of the aquifer and the clogging layer as:

$$K_E = \frac{\Delta x_{cl} + \Delta x_{aq}}{\frac{\Delta x_{cl}}{K_{cl}} + \frac{\Delta x_{aq}}{K_{aq}}} \quad (2)$$

where K (m d^{-1}) is the hydraulic conductivity and Δx (m) the flow distance through the clogging layer (cl) and the aquifer (aq). The equivalent hydraulic conductivity was further assessed using seepage devices (Figure 4(a)) adjusted for operation in flowing water

(Rosenberry 2008) as:

$$K_E = v_{\text{seep}} \frac{\Delta x}{\Delta h} \quad (3)$$

where Δh (m) is the mean difference in hydraulic head between the river and the aquifer (L5) during the measurement period and Δx (m) is the length of the flowpath between L5 and the river. The seepage flux v_{seep} (m d^{-1}) was estimated from changes in water volume in the plastic bag ΔV (m^3), the radius of the gauge R_s (m^2) and the time Δt (s) as:

$$v_{\text{seep}} = \frac{\Delta V}{\pi \Delta t R_s^2} \quad (4)$$

Seepage measurements were performed in October using 10 devices deployed on the river bed (Figure 4(b)) with an intake depth of 0.15 m. The seepage devices were run for 24 hours prior to the first measurement and visually inspected on every measurement occasion. The installation sites were free from boulders. The collection bags were tested for leakage and secured using barrels to protect them from water current and wave influence. The measurements were repeated up to five times at some of the locations to ensure good reproducibility.

The temporal variations in mean flux (q) per unit area ($m^3\,d^{-1}\,m^{-2}$, or m d^{-1}) between the river and well L5 and in the riparian zone between wells L5 and L25 were determined by Darcy's law, assuming 1-D flow:

$$q(t) = -K \frac{\Delta h}{\Delta x} \quad (5)$$

where Δh (m) is the difference in water level between locations and Δx (m) is the flow path between them.

The proportions of gaining and losing periods were determined, along with the number of shifts in water flow direction across the river bed (measured at 5 m distance from the MSL). These shifts were based on the difference between mean flow during 2 consecutive hours (a shift was made when the sign of the difference changed). Specific fluxes with an absolute value lower than 10^{-4} m d^{-1} were considered to be zero.

Temporal variations in the river water fraction (RWF, %) in the hyporheic zone were determined using the electrical conductivity of the river water (σ_r, μS cm^{-1}), the hyporheic zone (σ_h) and the groundwater (σ_{gw}) following Triska *et al.* (1989) as:

$$\text{RWF} = 100 \frac{\sigma_h - \sigma_{gw}}{\sigma_r - \sigma_{gw}} \quad (6)$$

Prerequisites for this relationship are that σ_{gw} and σ_r are fairly stable and that σ_h represents a mixture of σ_{gw} and σ_r. However, in this case the latter condition was not met, since σ_h was normally much higher than σ_{gw} and σ_r, possibly due to the presence of the clogging layer and increased residence time resulting in long-term interaction with the substrate and thereby promoting, for example, weathering. Therefore, σ_{gw} was replaced by a sinusoidal curve connecting the σ_r values without visible river water intrusions.

Heat conduction from the river water into the bed was used here as an indicator of water movement. A theoretical penetration depth d_{37} (m) of a conductive wave that represents 37% of the initial driving signal amplitude (Blasch *et al.* 2007) can be calculated based on the thermal diffusivity D_t ($m^2\,d^{-1}$) of the material, here the clogging layer, and the period of the wave φ (d^{-1}):

$$d_{37} = \sqrt{\frac{D_t \varphi}{\pi}} \quad (7)$$

The thermal signal from the surface water in the hyporheic zone would be observed farther away than determined by Equation (7) in the presence of advection. Penetration depth was determined for both daily and weekly pulses using a D_t value for the clogging layer of 0.11 m d^{-1} (Al Nakshabandi & Kohnke 1965).

RESULTS

Hydraulic conductivity

The clogging layer on the river bed had a mean hydraulic conductivity (± standard deviation) of 0.04 ± 0.01 m d^{-1} (Table 2), and was underlain by layers of variable conductivity (Figure 5). There was no statistical difference between the mean hydraulic conductivity of the aquifer measured with the direct-push

Table 2 | Hydraulic conductivity (m d^{-1} ± standard deviation) determined by different techniques for the clogging layer (K_{cl}) and the aquifer (K_{aq}), and equivalent hydraulic conductivity (K_E). Mean values in bold

Method	Number of samples	K_{cl}	K_{aq}	K_E
Grain size distribution and sedimentation	5	–		
Slug test; Hvorslev	3	–	0.13 ± 0.08	
Slug test; Bouwer and Rice	3	–	0.10 ± 0.09	
Direct-push piezometer	4	0.04 ± 0.01	0.24 ± 0.07	
		0.04 ± 0.01	**0.15 ± 0.08**[a]	0.13 ± 0.05
Seepage measurements				0.32 ± 0.19

[a]Mean standard deviation was estimated as square root of mean variance of individual standard deviations.

piezometer and the slug test (conf. int. =95%, $p = 0.056$, for number of samples, see Table 2).

The equivalent hydraulic conductivity based on the slug test for the aquifer and based on the direct-push piezometer for the clogging layer was estimated to be 0.13 ± 0.05 m d^{-1} (Equation (2)). The seepage measurements (Equation (3)) varied in space, revealing preferential upwelling zones within the reach. Devices No. 4–10 were considered to be most representative for the reach (Figure 4(b)) and were thus used for estimation of the equivalent hydraulic conductivity, resulting in $K_E = 0.32 \pm 0.19$ m d^{-1}.

Water fluxes

The monitoring period was characterised by two different types of river stage pattern. The first part (June–July) was dominated by daily stage oscillations (83% of the time) of low amplitude (mean 0.25 m), representing short-term river regulation. The latter part of the observation period was subjected to less frequent oscillations (waves with a one-week period were common during ≈35% of the time) but larger stage peaks (mean 0.5 m). The irregular river level fluctuations induced unnatural water flow pattern at the river-aquifer interface, although the reach continued to gain during 90% of the observation time (Figure 6). The riparian plain between wells L5 and L25 responded with a delay of 0.5–4.0 hours and a magnitude of fluxes one order lower than the flux across the river bed.

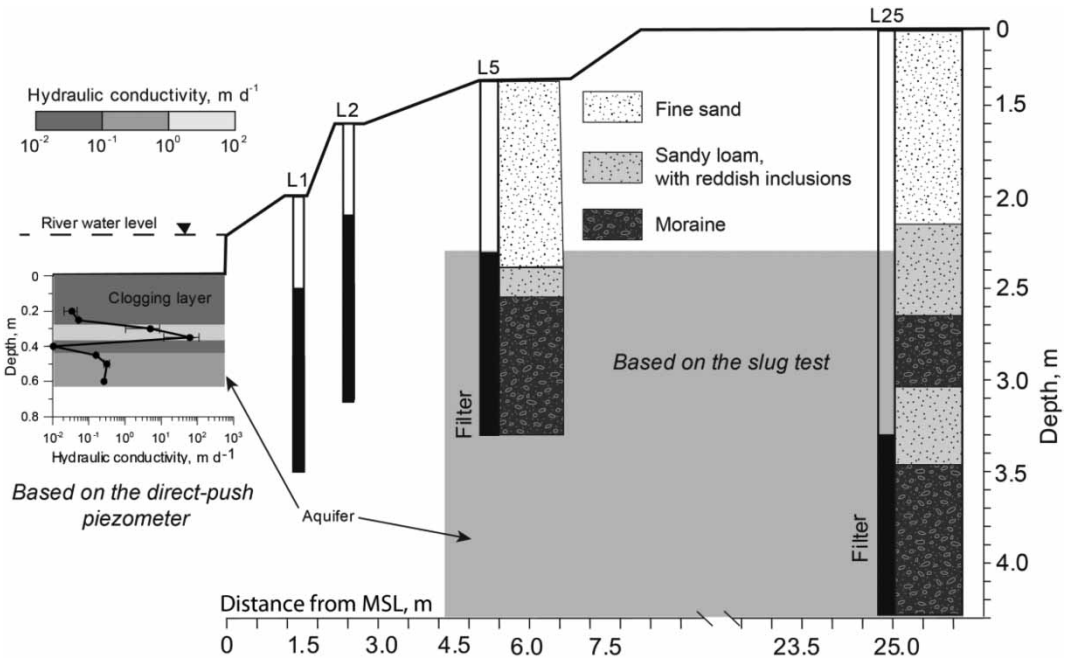

Figure 5 | Depth profiles of the sediment sequence and mean hydraulic conductivity values along the monitoring transect. Soil profiles based on visual inspection during drilling of L5 and L25 are shown.

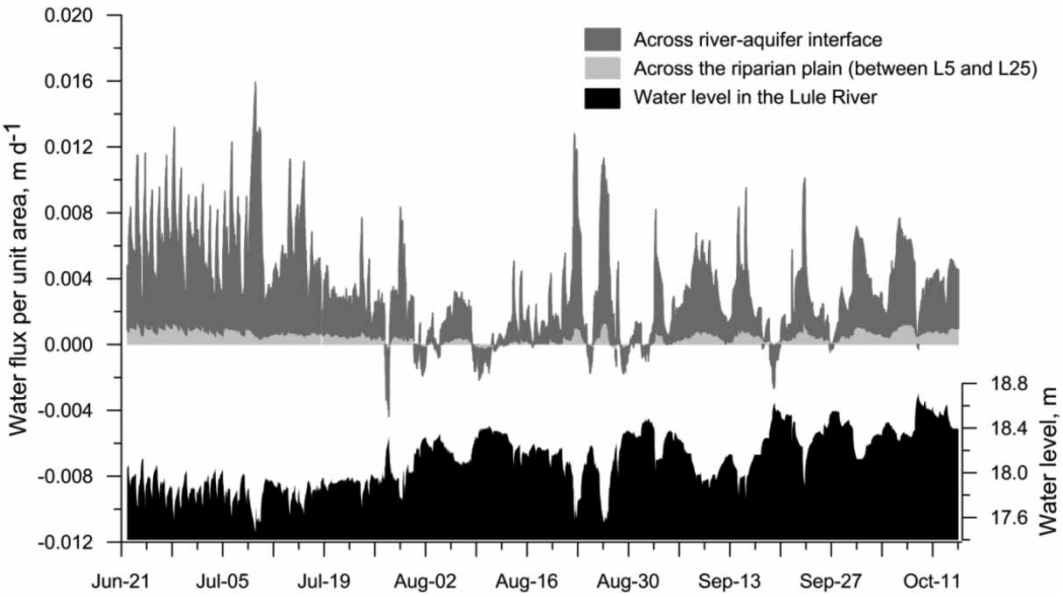

Figure 6 | Water level in the Lule River and orthogonal water flux across the river bed and the riparian plain during June–October 2012, based on the hydraulic gradient between well L5 and the river ($K_E = 0.13$ m d^{-1}) and between wells L5 and L25 ($K = 0.15$ m d^{-1}). Positive fluxes indicate flow towards the river.

The water fluxes across the river bed varied between −0.004 and 0.015 m d^{-1} (mean 0.003 m d^{-1}). Negative fluxes indicated infiltration of the river water into the aquifer and constituted ~3% of the total fluxes (or ~10% of the time) across the monitoring reach. During ~2% of the time, the flow across the river-aquifer interface was less than 10^{-4} m d^{-1} and was regarded as stagnant. The direction of flow across the river bed changed on average about twice per week, with a maximum of six changes per week (not all of which are visible in Figure 6 with the resolution used).

Seepage fluxes on 8 October varied laterally between 0.003 and 0.045 m d^{-1} (Figure 7), with the higher values recorded at the sandy/gravel outwash upstream and closer to the MSL and the lower values in deeper and vegetated areas (Figure 4(b)). All seepage fluxes were positive during the measurement occasion. The mean flux from devices No. 4–10 (closest to the monitoring transect) was 0.006 m d^{-1}, while that obtained from the hydraulic gradient (Equation (5)) during the same period was 0.003 m d^{-1}.

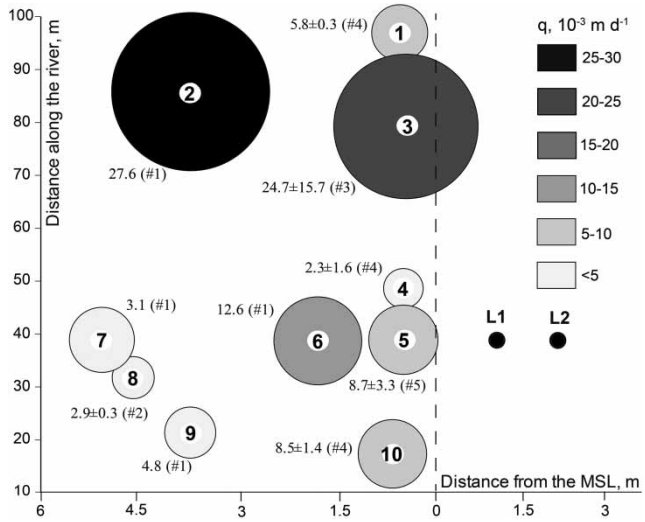

Figure 7 | Lateral variations in seepage flux (10^{-3} m d^{-1} ± standard deviation) with number of measurements and location of wells L1 and L2 along the monitoring reach.

Groundwater temperature as an indicator of river-groundwater exchange

The temperature profile in the river bed (for location see Figure 2) showed that river water heat wave propagation was visible down to 0.8 m depth (Figure 8). Around 25% of the weekly and 21% of the daily temperature amplitude in the river reached 0.2 m depth (calculated based on the distribution of daily temperature amplitudes along the depth profile). A similar depth (0.2 m) was obtained for penetration of 37% of the diurnal temperature signal (Equation (7)). These results suggest mainly conductive transfer of heat from the river into

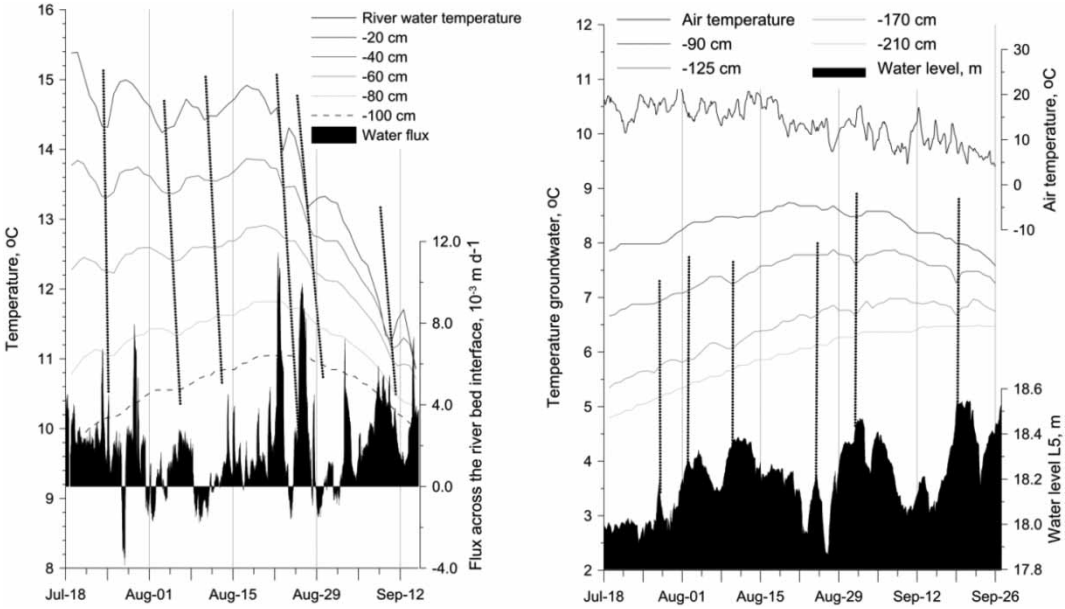

Figure 8 | Daily mean temperature profiles in the river bed 2 m (left) and inland 5 m from the MSL (right). Lines across the time-series connecting temperature minima to groundwater stages demonstrate the effects of conduction in the river bed and upwelling of colder groundwater at L5 during rising river levels. Note that short-term variations are not visible.

the aquifer at the observation site, with a time lag of up to 1 week. The temperature monitoring in L1 was similar, demonstrating no river water intrusion (data not shown).

Groundwater temperature in the depth profile 5 m inland from the MSL had a maximum in August for shallow horizons and in September for deep horizons. No influence of river water was detected, but several simultaneous temperature drops at depths from −90 to −170 cm were observed during the periods of rising river levels (Figure 9), which indicates upwelling of deeper colder groundwater.

Electrical conductivity

The electrical conductivity in the river varied between 19 and 25 μS cm^{-1}, with slightly higher values during July–September. The values in the groundwater wells at 5 and 25 m distance were more than twice as large and also fairly stable (L5: 40–80 μS cm^{-1}; L25: 50–70 μS cm^{-1}) (Figure 9). In the wells closest to the river (L1, L2), electrical conductivity ranged between 70 and 130 μS cm^{-1} and depended on the regulation pattern, i.e. with short-term regulation during summer and long-term regulation later in the year.

During the summer (June–July), when daily river discharge fluctuations prevailed, most of the changes in electrical conductivity measured in L1 were a function of the gradient between the river and the groundwater measured in L5. Electrical conductivity decreased with decreasing gradient, i.e. rising river water level, with a delay of 3–5 hours.

In August–October, with extended discharge maxima, an inverse relationship was found between the gradient and electrical conductivity. A pattern similar to that observed during summer was seen only when sufficiently sharp river level fluctuations occurred, which was rare during late summer and early autumn.

Occasional intrusion of surface water into the hyporheic zone resulted in the mean proportion of surface water (Equation (6)) being 31% in L1, 14% in L2 and 2% in L5.

DISCUSSION

The Lule River has been regulated for almost a century (Forsgren 1990). Obstruction of the river by dams occurred stepwise and has been shown to influence the river water composition and the bottom sediments (Sferratore *et al.*

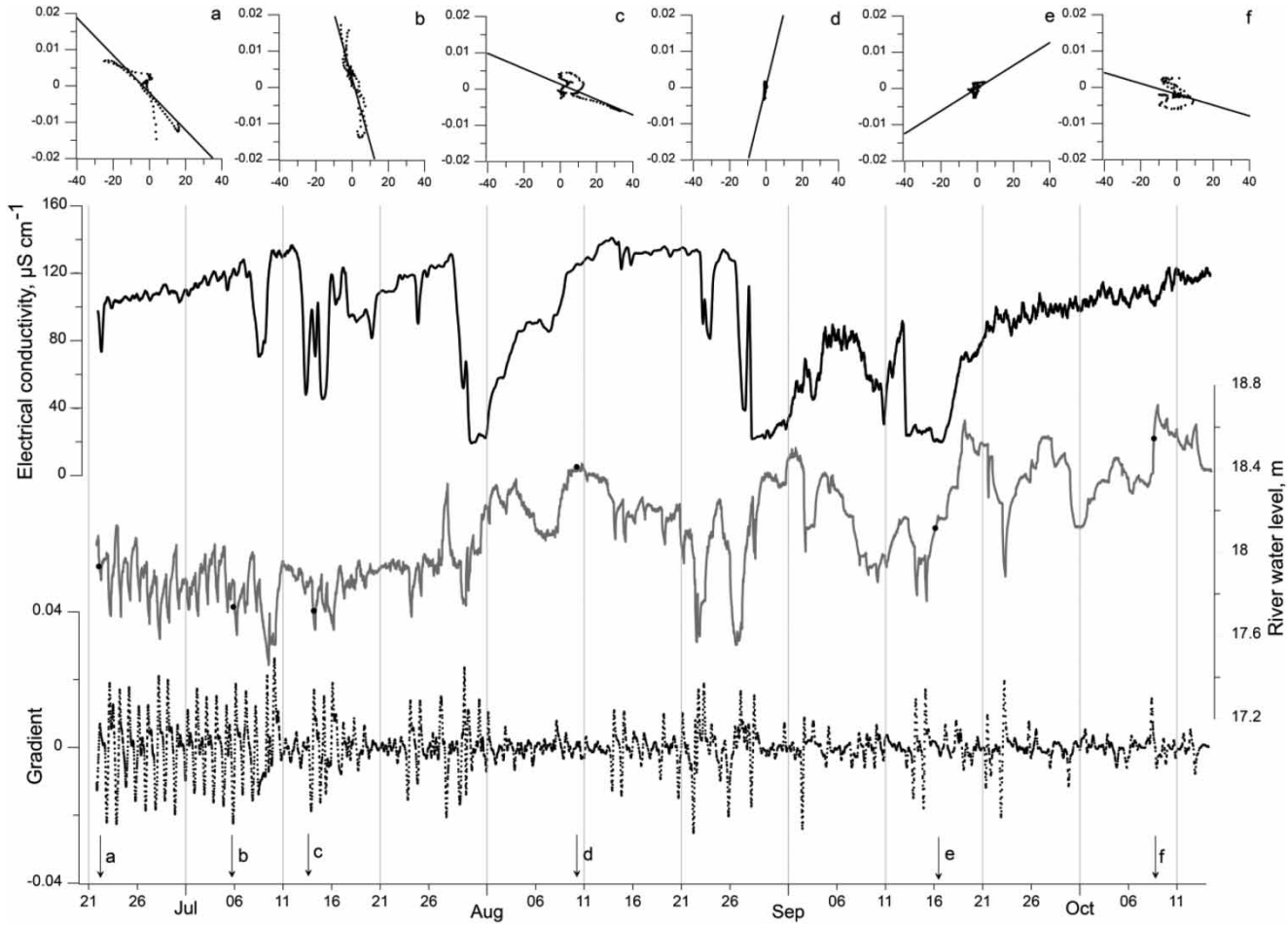

Figure 9 | Variations in electrical conductivity, orthogonal gradient between L5 and the river (LR) and river water level during the observation period. Scatter plots of changes in electrical conductivity (x-axis) versus changes in the gradient (y-axis) are shown for selected daily occasions (a–f). Negative correlations represent occasions with abrupt changes in the gradient, while positive correlations were common for days with gradual changes in the gradient.

2008; Smedberg *et al*. 2009; Siergieiev 2013), which has resulted in deterioration of the river-aquifer interaction.

Heterogeneity of hyporheic zone

At the monitoring site used in the present study, the river bed was partially covered with a dense, 0.3 m thick clogging layer composed of fine sediments, with hydraulic conductivity of 0.04 ± 0.01 m d^{-1}. Down to 0.7 m depth, highly and poorly permeable strata occurred, indicating inhomogeneity along the hyporheic flowpath, which agrees well with the findings from other regulated rivers (Hancock & Boulton 2005; Hanrahan 2008; Gibbins *et al*. 2009). The spatial distribution of the clogging layer and its thickness were not studied in detail, resulting in rather large uncertainties in the calculated water fluxes. The presence of layers and sub-areas with deficient conductivity increased residence times and created a complex flowpath, thus having impacts on the biogeochemistry of the hyporheic zone. In contrast, in unregulated boreal river systems (e.g. the neighbouring Kalix River in Northern Sweden), the river bed is usually flushed free of fines during floods.

According to our seepage measurements, the equivalent hydraulic conductivity of the Lule River bed varied spatially from 0.12 to 1.74 m d^{-1}. These variations could be due to, for example, uneven thickness (or absence) of the clogging layer or variations in river bed topography and/or vertical hydraulic gradient (not measured). Higher equivalent hydraulic conductivity was observed on vegetation-free areas and lower values farther away from the shore and at the sites

with aquatic plants (macrophytes closer to the shore and Chara sp. in deeper waters). This is in agreement with findings reported by Rosenberry *et al.* (2000). Although the representativeness of the seepage measurements could not be fully guaranteed, the data obtained were verified by application of several seepage devices over a small area.

Water flux across the river bed

The fluxes estimated using hydraulic conductivity from the piezometer and slug tests were only half those obtained using the seepage devices. Neither the slug nor piezometer tests, with their scarce coverage, could describe all the heterogeneity of the subsurface. The higher fluxes obtained with the seepage devices, which had better exposure over the monitored stretch, suggest underestimation of fluxes based on the equivalent hydraulic conductivity. Therefore, the latter method gave smaller fluxes and thus smaller differences compared with unperturbed systems, which would increase if larger K_E were applied. Correct levelling of the water level sensors was found to improve the quality of the flux estimates and was thus performed twice. However, estimates of the gradient based on the 5 m distance could still have concealed small-scale changes in flow direction and orthogonal fluxes.

Orthogonal fluxes from the river towards the aquifer were estimated to be 3% of the total fluxes, whereas those for a similar large hydropower-regulated river (the Colorado River) are reported to be around 20% (Sawyer *et al.* 2009). Absence of a clogging layer and higher hydraulic conductivity of the river bed at their site could partly explain this difference (Dr A.H. Sawyer, University of Kentucky, USA, personal communication, May 2012). For the pristine Kalix River, with its gradual discharge variations, the fluxes remain directed towards the river during the entire summer, since the groundwater levels were always higher than the river water levels (based on the measurements during 2010–2012; see also Siergieiev (2013)).

Multi-dimensions of the hyporheic zone

Most of the observations in this study were limited to one (or two) dimensions and could possibly have overlooked the real nature of processes occurring in 4-D (x, y, z and time). The gradient (dh/dx) from the transect only provided an indication of orthogonal fluxes, while the seepage measurements included all flux components (x, y and z). The specific groundwater flux along the river (based on the local gradient of the river surface 1.7×10^{-5}, from elevation at upstream and downstream dams) using the hydraulic conductivity of the most permeable layer (100 m d^{-1}) and the arithmetic mean of hydraulic conductivity of the river bed (0.15 m d^{-1}) (Figure 4 and Table 2) was 4.0×10^{-3} and 6.0×10^{-6} m d^{-1}, respectively. In comparison, the mean specific flux orthogonal to the river was 3.0×10^{-3} m d^{-1}. Note that the specific flux values used here were defined as flux divided by area, without taking effective porosity into account, which would be necessary as regards flow distances and residence times.

The gradient along rivers is usually smaller for regulated than for pristine rivers (e.g. for the nearby unregulated Kalix River the lateral gradient is 4.0×10^{-5} at the same distance from the mouth as in the current study). This is because the steepest parts of regulated rivers are replaced by tunnels and turbines, so fluxes parallel to the channel can be expected to be smaller. Consideration of all existing dimensions in future studies would increase the chances of revealing the highly variable character of hyporheic processes.

Temperature

The heat exchange between the river and the aquifer was of a conductive nature, according to temperature monitoring. No relationship was found between the heat wave propagation into the river bed and the river stage fluctuations. In contrast, in the Colorado River, temperature pulses have been observed down to 1 m in the river bed, with hydraulic conductivity of 15.7 m d^{-1} and daily river level variations of >1.5 m (Gerecht *et al.* 2011). Therefore, heat propagation into the hyporheic zone appears to be highly dependent on the permeability of the river bottom and the magnitude of the water level variations.

Electrical conductivity

Natural discharge variations in unregulated systems form a hyporheic zone with slow variations in size, temperature and water quality. The hyporheic zone in regulated rivers

is characterised by irregular water fluxes forced across the river bed, which maintains temporally unstable size and water quality of the hyporheic zone (Arntzen *et al.* 2006; Sawyer *et al.* 2009).

The effects of regulation on the electrical conductivity of the hyporheic zone in the Lule River differed depending on the regulation pattern and season. Based on the relationship between the pressure gradient and electrical conductivity, the hyporheic water quality of the Lule River is mainly controlled by the river stage fluctuation during most of the summer and by hillslope processes during autumn.

The increased electrical conductivity in L1 and L2 compared with the surrounding groundwater suggests the presence of a 'hotspot', a relatively immobile area in the hyporheic zone with excessive reaction rates (McClain *et al.* 2003). The presence of a clogging layer and reduced hyporheic exchange increase hyporheic retention time and thus enhance weathering reactions and microbial metabolism (Gerla 2013). In the unregulated Kalix River, the river bottom is free from clogging, suggesting active hyporheic exchange (Siergieiev 2013).

Fraction of river water in neighbouring wells

The experimental set-up used by Sawyer *et al.* (2009) was fairly similar to that used here and showed that RWF was 25% in a well 5 m from the Colorado River channel (≈600 $m^3 s^{-1}$, daily level variations ±1.5 m, no clogging layer), whereas the corresponding value for the Lule River (≈500 $m^3 s^{-1}$, level variations ±0.25 m daily, with clogging layer) was 2%. Estimates for the unregulated Kalix River (≈300 $m^3 s^{-1}$, no large daily level variations, no clogging layer) indicate approximately 25% RWF in a well 2 m from the channel (based on unpublished data collected during 2010–2012, see also Siergieiev (2013)). Thus, the variations between rivers may be large and are highly dependent on local hydrogeological conditions. In natural systems, the river water volume in the subsurface layers is more stable over time than in regulated rivers.

Data availability

Information regarding the high variability in hyporheic water processes has until recently been lacking due to lack of suitable equipment for continuous *in situ* monitoring (Malcolm *et al.* 2009). *In situ* online monitoring with simultaneous deployment of several high resolution techniques is advantageous when mapping hyporheic processes at various scales.

Apart from temperature and electrical conductivity, as used in this and several other studies, dissolved oxygen (Soulsby *et al.* 2009), electrochemical/optical/reactive surface sensors (Hanrahan *et al.* 2004), fibre-optics (Vogt *et al.* 2010), infrared imaging (Korkka-Niemi *et al.* 2012), electrical resistivity (Cardenas & Markowski 2011), ground-penetrating radar (Brosten *et al.* 2009), acoustic imaging (Bianchin *et al.* 2011), etc., have been successfully employed for studying hyporheic processes.

Future studies in this field must combine several different techniques with dense coverage in both the vertical and horizontal directions. Knowledge gaps about the distribution and development of a clogging layer in hydropower-regulated rivers can be filled by understanding sediment transport in regulated rivers.

In this study, geochemical parameters were also measured and will be used in a later study to further assess the hyporheic processes in the regulated Lule River and the neighbouring unregulated Kalix River. The results presented here have implications for the biogeochemical functioning of the hyporheic zone in hydropower-regulated rivers and provide a basis for future geochemical research to assess the effects of river regulation on river-aquifer exchange in boreal environments.

CONCLUSIONS

Hyporheic exchange in the boreal hydropower-regulated Lule River in Northern Sweden was studied during one ice-free season using an orthogonal transect. As a result of regulation, river-aquifer connectivity and hyporheic exchange were altered as follows:

1. Measurements of hydraulic conductivity of the river bed revealed the presence of a clogging layer. Colmation was most likely promoted by a diminished spring peak and the presence of a short-term regulation pattern, i.e.

daily discharge fluctuation with amplitude ±0.25–0.5 m at the study site.

2. The Lule River recharged the aquifer during 10% of the time, which constituted 3% of the total exchange volume, while unregulated rivers in Northern Sweden generally remain gaining throughout the year.
3. Daily stage fluctuations decreased the specific orthogonal fluxes across the river-aquifer interface, and during 2% of the time the fluxes were negligible ($<10^{-4}$ m d^{-1}).
4. Electrical conductivity in the hyporheic zone varied temporally due to reversals of flow across the river-aquifer interface. The mean proportion of river water in the subsurface was 31, 14 and 2% at 1, 2 and 5 m inland, respectively, indicating the extent of hyporheic exchange.
5. Electrical conductivity of the hyporheic water was controlled by river discharge during summer and by hillslope processes during the rest of the observation period.
6. In contrast to electrical conductivity, temperature changes had no effect on the hyporheic zone of the fluxes across the river bed, suggesting conductive heat transfer between the river and the aquifer.

ACKNOWLEDGEMENTS

This work forms part of the GENESIS project on groundwater systems (www.thegenesisproject.eu), funded by the European Commission 7FP contract 226536. The Kempe foundation and Formas (project number 242-210-1187) are greatly acknowledged for additional financial support. We are also much indebted to P. Ala-Aho and P. Rossi, University of Oulu, Finland, for the loan of the direct-push piezometer for measuring hydraulic conductivity.

REFERENCES

Al Nakshabandi, G. & Kohnke, H. 1965 Thermal conductivity and diffusivity of soils as related to moisture tension and other physical properties. *Agr. Meteorol.* **2**, 271–279.

Aneblom, T., Thunholm, B., Rurling, S. & Gierup, J. 2005 *Beskrivning till kartan över grundvattnet i Norrbottens län [Description of the groundwater map in Norrbotten county].* SGU, Uppsala.

Arntzen, E. V., Geist, D. R. & Dresel, P. E. 2006 Effects of fluctuating river flow on groundwater/surface water mixing in the hyporheic zone of a regulated, large cobble bed river. *Riv. Res. Appl.* **22**, 937–946.

Bianchin, M. S., Smith, L. & Beckie, R. D. 2011 Defining the hyporheic zone in a large tidally influenced river. *J. Hydrol.* **406**, 16–29.

Blasch, K. W., Constantz, J. & Stonestrom, D. A. 2007 Thermal methods for investigating ground-water recharge. *US Geol. Surv. Prof. Pap.* **1703**, 353–376.

Blaschke, A. P., Steiner, K. H., Schmalfuss, R., Gutknecht, D. & Sengschmitt, D. 2003 Clogging processes in hyporheic interstices of an impounded river, the Danube at Vienna, Austria. *Int. Rev. Hydrobiol.* **88**, 397–413.

Bouwer, H. 1989 The Bouwer and Rice slug test – an update. *Ground Water* **27**, 304–309.

Brosten, T. R., Bradford, J. H., McNamara, J. P., Gooseff, M. N., Zarnetske, J. P., Bowden, W. B. & Johnston, M. E. 2009 Multi-offset GPR methods for hyporheic zone investigations. *Near Surf. Geophys.* **7**, 244–257.

Brunke, M. & Gonser, T. 1997 The ecological significance of exchange processes between rivers and groundwater. *Freshw. Biol.* **37**, 1–33.

Calles, O., Nyberg, L. & Greenberg, L. 2007 Temporal and spatial variation in quality of hyporheic water in one unregulated and two regulated boreal rivers. *Riv. Res. Appl.* **23**, 829–842.

Cardenas, M. B. & Markowski, M. S. 2011 Geoelectrical imaging of hyporheic exchange and mixing of river water and groundwater in a large regulated river. *Environ. Sci. Technol.* **45**, 1407–1411.

Directive 2006/118/EC 2006 Directive 2006/118/EC of the European Parliament and of the Council of 12 December 2006 on the protection of groundwater against pollution and deterioration. *Official J. Eur. Union, L* **372** (19).

Dole-Olivier, M. J. 2011 The hyporheic refuge hypothesis reconsidered: a review of hydrological aspects. *Mar. Freshw. Res.* **62**, 1281–1302.

Dynesius, M. & Nilsson, C. 1994 Fragmentation and flow regulation of river systems in the northern third of the world. *Science* **266**, 753.

Forsgren, N. 1990 *Den effektfulla älven: stänk från Luleälvens kraftfulla historia [The powerful river. A splash from the Lule River great history].* Vattenfall, Luleå.

Francis, B. A., Francis, L. K. & Cardenas, M. B. 2010 Water table dynamics and groundwater–surface water interaction during filling and draining of a large fluvial island due to dam-induced river stage fluctuations. *Water Resour. Res.* **46**, W07513.

Geist, D. R., Arntzen, E. V., Murray, C. J., McGrath, K. E., Bott, Y. J. & Hanrahan, T. P. 2008 Influence of river level on temperature and hydraulic gradients in chum and fall Chinook salmon spawning areas downstream of Bonneville Dam, Columbia River. *N. Am. J. Fish. Manage.* **28**, 30–41.

Gerecht, K. E., Cardenas, M. B., Guswa, A. J., Sawyer, A. H., Nowinski, J. D. & Swanson, T. E. 2011 Dynamics of hyporheic flow and heat transport across a bed-to-bank continuum in a large regulated river. *Water Resour. Res.* **47**, W03524.

Gerla, P. 2013 Can pH and electrical conductivity monitoring reveal spatial and temporal patterns in wetland geochemical processes? *Hydrol. Earth Syst. Sc. Disc.* **10**, 699–728.

Gibbins, C., Soulsby, C. & Malcolm, I. 2009 Impact of artificial freshet releases on channel hydraulics and the hyporheic zone of a gravel bed river. *Geophys. Res. Abs.* **11**, 10800.

Hancock, P. J. 2002 Human impacts on the stream-groundwater exchange zone. *Environ. Manage.* **29**, 763–781.

Hancock, P. & Boulton, A. 2005 The effects of an environmental flow release on water quality in the hyporheic zone of the Hunter River, Australia. *Hydrobiologia* **552**, 75–85.

Hanrahan, T. P. 2008 Effects of river discharge on hyporheic exchange flows in salmon spawning areas of a large gravel-bed river. *Hydrol. Process.* **22**, 127–141.

Hanrahan, G., Patil, D. G. & Wang, J. 2004 Electrochemical sensors for environmental monitoring: design, development and applications. *J. Environ. Monit.* **6**, 657–664.

Howard, K., Maier, H. & Mattson, S. 2006 Ground-surface water interactions and the role of the hyporheic zone. In: *Groundwater and Ecosystems. NATO Science Series IV Earth and Environmental Sciences*, vol. 70 (A. Baba, K. W. F. Howard & O. Gunduz, eds). Springer, The Netherlands, pp. 131–143.

Humborg, C., Smedberg, E., Medina, M. R. & Mörth, C. M. 2008 Changes in dissolved silicate loads to the Baltic Sea – The effects of lakes and reservoirs. *J. Mar. Syst.* **73**, 223–235.

Hvorslev, M. J. 1951 Time lag and soil permeability in ground-water observations. *Waterways Exp. Stat. Bull. US Army* **36**, 1–50.

Jansson, R., Nilsson, C. & Renöfält, B. 2000 Fragmentation of riparian floras in rivers with multiple dams. *Ecology* **81**, 899–903.

Klöve, B. 2008 GENESIS, an integrated research project to support groundwater systems management. *EU Groundwater Policy Developments Conference*. UNESCO, Paris, France.

Korkka-Niemi, K., Kivimäki, A. L., Lahti, K., Nygård, M., Rautio, A., Salonen, V. P. & Pellikka, P. 2012 Observations on groundwater-surface water interactions at River Vantaa, Finland. *Manage. Environ. Qual. Int. J.* **23**, 222–231.

Maier, H. S. & Howard, K. W. F. 2011 Influence of oscillating flow on hyporheic zone development. *Ground Water* **49**, 830–844.

Malcolm, I., Soulsby, C., Youngson, A. & Tetzlaff, D. 2009 Fine scale variability of hyporheic hydrochemistry in salmon spawning gravels with contrasting groundwater-surface water interactions. *Hydrogeol. J.* **17**, 161–174.

McClain, M. E., Boyer, E. W., Dent, C. L., Gergel, S. E., Grimm, N. B., Groffman, P. M., Hart, S. C., Harvey, J. W., Johnston, C. A. & Mayorga, E. 2003 Biogeochemical hot spots and hot moments at the interface of terrestrial and aquatic ecosystems. *Ecosystems* **6**, 301–312.

McDonald, A. K., Sheng, Z., Hart, C. R. & Wilcox, B. P. 2012 Studies of a regulated dryland river: surface–groundwater interactions. *Hydrol. Proc.* **27**, 1819–1828.

Murray, B. B. R., Zeppel, M. J. B., Hose, G. C. & Eamus, D. 2008 Groundwater-dependent ecosystems in Australia: It's more than just water for rivers. *Ecol. Manage. Restor.* **4**, 110–113.

Nilsson, C., Reidy, C. A., Dynesius, M. & Revenga, C. 2005 Fragmentation and flow regulation of the world's large river systems. *Science* **308**, 405.

Nogaro, G., Datry, T., Mermillod-Blondin, F., Descloux, S. & Montuelle, B. 2010 Influence of streambed sediment clogging on microbial processes in the hyporheic zone. *Freshwat. Biol.* **55**, 1288–1302.

Raab, B. & Vedin, H. 1995 *Climate, Lakes and Rivers*. Swedish National Atlas. Swedish Meteorological and Hydrological Institute – SMHI, Sweden.

Rehg, K. J., Packman, A. I. & Ren, J. 2005 Effects of suspended sediment characteristics and bed sediment transport on streambed clogging. *Hydrol. Process.* **19**, 413–427.

Renöfält, B., Jansson, R. & Nilsson, C. 2010 Effects of hydropower generation and opportunities for environmental flow management in Swedish riverine ecosystems. *Freshwat. Biol.* **55**, 49–67.

Ronkanen, A. K. & Klove, B. 2005 Hydraulic soil properties of peatlands treating municipal wastewater and peat harvesting runoff. *Suo* **56**, 43–56.

Rosenberry, D. O. 2008 A seepage meter designed for use in flowing water. *J. Hydrol.* **359**, 118–130.

Rosenberry, D. O., Striegl, R. G. & Hudson, D. C. 2000 Plants as indicators of focused ground water discharge to a northern Minnesota lake. *Ground Water* **38**, 296–303.

Sawyer, A. H., Bayani Cardenas, M., Bomar, A. & Mackey, M. 2009 Impact of dam operations on hyporheic exchange in the riparian zone of a regulated river. *Hydrol. Process.* **23**, 2129–2137.

Sferratore, A., Billen, G., Garnier, J., Smedberg, E., Humborg, C. & Rahm, L. 2008 Modelling nutrient fluxes from sub-arctic basins: comparison of pristine vs. dammed rivers. *J. Mar. Syst.* **73**, 236–249.

Siergieiev, D. 2013 Impact of hydropower regulation on river water geochemistry and hyporheic exchange. Licentiate thesis, 91.

Smedberg, E., Humborg, C., Jakobsson, M. & Mörth, C. M. 2009 Landscape elements and river chemistry as affected by river regulation – a 3-D perspective. *Hydrol. Earth Syst. Sc.* **13**, 1597–1606.

Soulsby, C., Malcolm, I., Tetzlaff, D. & Youngson, A. 2009 Seasonal and inter-annual variability in hyporheic water quality revealed by continuous monitoring in a salmon spawning stream. *River Res. Appl.* **25**, 1304–1319.

Soulsby, C., Malcolm, I. & Youngson, A. 2001 Hydrochemistry of the hyporheic zone in salmon spawning gravels: a preliminary assessment in a degraded agricultural stream. *Regul. Rivers Res. Manage.* **17**, 651–665.

Triska, F. J., Kennedy, V. C., Avanzino, R. J., Zellweger, G. W. & Bencala, K. E. 1989 Retention and transport of nutrients

in a third-order stream: channel processes. *Ecology* **70**, 1877–1892.

Vogt, T., Schneider, P., Hahn-Woernle, L. & Cirpka, O. A. 2010 Estimation of seepage rates in a losing stream by means of fiber-optic high-resolution vertical temperature profiling. *J. Hydrol.* **380**, 154–164.

Wondzell, S. M. 2011 The role of the hyporheic zone across stream networks. *Hydrol. Proc.* **25**, 3525–3532.

Zhao, T., Richards, K. S., Xu, H. & Meng, H. 2012 Interactions between dam-regulated river flow and riparian groundwater: a case study from the Yellow River, China. *Hydrol. Proc.* **26**, 1552–1560.

First received 10 January 2013; accepted in revised form 11 June 2013. Available online 25 July 2013